# Properties of Piezoelectric Tube Actuators for use in a Fiber Positioner for a Spectroscopic Telescope

Undergraduate Honor Thesis

Presented to

The Faculty of the School of Arts and Science

Brandeis University

Undergraduate Program in Physics

James Bensiger, and Marcelle Soares-Santos, Advisors

In partial fulfillment of the requirements of the degree of

Bachelor of Science

by

Guadalupe Duran

May 2020

# Signatures

James Bensinger, Committee Member — Date

Marcelle Soares-Santos, Committee Member — Date

# Acknowledgements

I would like to thank James Bensinger and Marcelle Soares-Santos for being my thesis advisors and for their help and guidance throughout this project. I would like to thank Kevan Hashemi for his constant feedback and assistance along every step of the way. I would also like to thank Anushka Shrivastava for the work she did in getting this project started, and for helping me along the way. Lastly, I would like to thank Richard Studly and Kimika Arai for helping me build essential components for this project and Jesse Held for his help with Latex.

**Abstract**

Obtaining spectroscopic data from astronomical objects will always be a goal of astrophysics. Recent photometric surveys have greatly increased the number of objects for which to obtain spectra. To keep up with this increase of photometric data, we need a fiber positioning system that is capable of efficiently taking the spectrum of hundreds of millions or even a billion sources. Such a system would need to be capable of imaging many objects at once, which requires many fibers in the focal plane and a rapid repositioning time. We studied the effects of hysteresis, creep, and temperature on the positioning precision of a piezoelectric tube actuator for use in a fiber positioning system. We investigated several methods of mitigating both hysteresis and creep and found the results encouraging; however, further tests are necessary to verify their effectiveness.

# 1 Introduction

Current and future telescopes and optical surveys have greatly increased the number of objects astronomers have observed and catalogued. However, spectroscopy provides insight into the universe that other methods of astronomy cannot. For instance, within our own galaxy, spectroscopy can provide chemical composition and radial velocity information about stars in the Milky Way [4]. We can use spectroscopy to study galaxy formation at cosmic noon, and it even has potential to provide insight towards the mass of the neutrino [15]. For cosmology, spectroscopy can provide accurate redshift measurements [4]. Thus a spectroscopic instrument able to observe both low redshift objects (in the dark energy dominated era) and high redshift objects (in the matter dominated era) will improve our understanding of dark energy by constraining large classes of theories, testing possible modifications to general relativity, and improving constraints on inflation [11]. This is done with spectroscopy directly, by direct observation, and indirectly by using spectroscopic survey data to train algorithms that use machine learning to find the photometric redshift from photometric surveys [11]. Previous surveys, such as the Sloan Digital Sky Survey have shown the benefits of combining imaging surveys with multiple-object spectroscopic data [4].

To achieve these scientific goals, we need a spectroscopic instrument capable of taking the spectra of upwards of several hundred billion objects. One tool that will allow us to do so is a fiber positioner with a large number of fibers. While this number is dependent upon the telescope the fiber positioner would be installed upon, the following are some current projects and their estimations for fiber number. The Maunakea Spectroscopic Explorer, a spectroscopic experiment to be located in Hawaii, will have 4332 fibers feeding low, high, and moderate resolution spectrographs [15]. The Large Synoptic Survey Telescope (LSST), currently under

construction in Chile, is another telescope nearing completion. Currently, the community is discussing the possibility of constructing and adding a spectroscopic instrument to the LSST for future work. While there is much left to be considered, it is estimated that there would need to be between 30,000 to 40,0000 fibers in the 3200 $cm^2$ focal plane [14] [3].

It is important that whatever fiber positioning system is constructed for such telescopes is compact, reliable, and with a short down time while repositioning fibers. This will aid in acquiring the spectra for the large number of targets in an efficient time frame. The piezoelectric tube actuator we study in this paper for potential use in a fiber positioner is just one of many fiber positioning systems that are currently in use or proposed.

## 1.1 Fiber Positioning Systems

There are many different fiber positioning systems that have been used historically and currently to assist in performing spectroscopy. We shall briefly discuss three different designs: the tilting spine, the twirling post, and Starbugs.

### 1.1.1 Tilting Spine

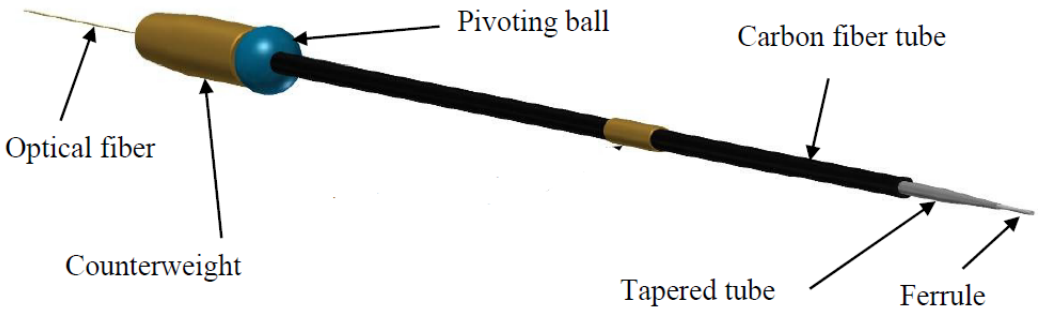


Figure 1: Diagram of a Tilting Spine, indicating the pivoting ball, the optical fiber, and the carbon fiber tube [12].

Tilting spine technology has been used since 2007 on the SUBARU telescope. An improved tilting spine design with greater efficiency will be used on 4MOST, a spectroscopic survey instrument for the VISTA telescope, with approximately 2,500 fibers [12] [13]. This technology will also be used in the Sphinx fiber positioner for Maunakea Spectroscopic Explorer, utilizing 4332 fibers [13].

A tilting spine has two parts, the base and the spine. The base consists of a piezoceramic tube with four electrodes in quadrants on the outside. It is connected to a cup on top which contains a small magnet. The spine consists of a tube containing the fiber, which is passed through a steel ball. The ball is held magnetically in the cup [12]. The tilting spine can be driven in steps as small as a few microns, to as large as approximately 50 microns. The step size is set by the amplitude of the drive signal. This drive signal is a sawtooth waveform, which uses voltages up to 200V. When this waveform is applied to the piezoceramic tube the resulting stick-slip friction between the cup and ball allows the spine to be tilted in any direction [12].

### 1.1.2 Twirling Post

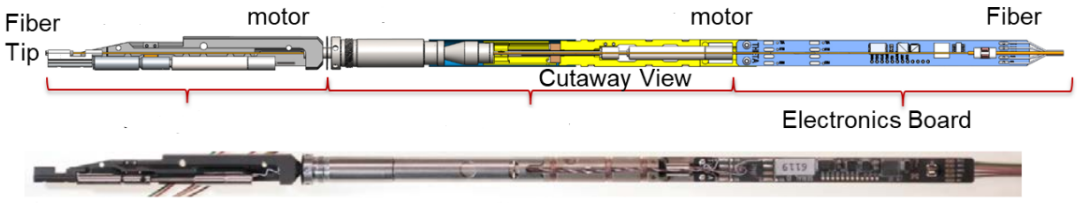


Figure 2: A diagram (top) and photograph(bottom) of a twirling post. The location of the motors are indicated on the diagram [9].

Twirling posts are robotic fiber positioners used on DESI (Dark Energy Spectroscopic Instrument). They use a two-degree-of-freedom system which utilizes two DC brushless gear motors, among many other components, to move individual optical fibers in the focal plane with a precision of 5 microns. DESI will use 5,000 of these fiber positioners [9] [10]. Each fiber positioner has a 12mm patrol region and there are 10.4mm between robots. Because of this overlap between the patrol regions of each fibers, potential collisions must be considered when selecting the targets [10]. The fiber positioner is less precise on large moves, so the fiber positioner software uses an iterative process to position the fiber tips. Once the initial move is made, the system illuminates all of the fiber tips and images them with a field of view camera. Then, the software measures the location of each fiber relative to the target location and determines if any correction is necessary, and if so, repeats the process [10]. This is a relatively quick process, and all fibers are in position in less than 120s [9].

### 1.1.3 Starbugs

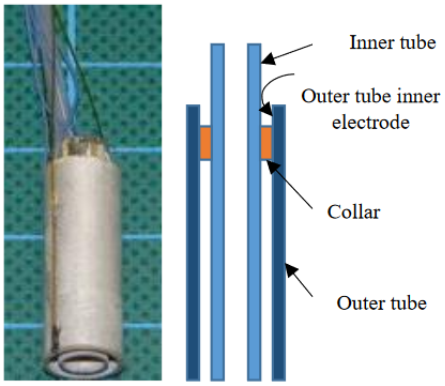


Figure 3: Photograph of a Starbug (left), and a cut away diagram of the two piezo-ceramic tubes, showing their configuration (left) [1].

Starbugs are 9mm diameter miniaturized piezoelectric walking robots designed at the Australian Astronomical Observatory. They can be operated simultaneously to position optical fibers across a telescope's focal plane [1]. Starbugs consist of two concentric piezo-ceramic tubes and necessary support wires. They are held to glass on the focal surface by a slight vacuum, and walk with a step size of approximately 1 micron [1]. Starbugs were tested and used on the TAIPAN instrument, which is a multi-object parallel-positioning fiber-optic spectrograph designed for the UK Schmid Telescope in Australia. TAIPAN will use 300 Starbugs to demonstrate functionality for future use on MANIFEST, which is proposed for the Giant Magellan Telescope [1].

## 1.2 System Requirements

We investigated several properties of a piezoelectric tube actuator to determine its usefulness in a potential fiber positioning system for a spectroscopic telescope. Any fiber positioning system constructed for such telescopes must be compact, reliable, and have a short downtime between repositioning the fibers. We must be able to position the tip of the fiber reliably to 10 microns, and maintain it at that position to within 10 microns over the period of an hour (the approximate time of an observation). The main component of the fiber positioners we studied is a piezoelectric tube actuator, also referred to as a piezo. The piezo mount board we used has a fiber tip to fiber tip distance of 5.08mm, demonstrating compactness. The tests we performed on the piezo in this study were to help us determine if we could meet the precision requirement of positioning the fiber to within 10 microns.

# 2 Experimental Design

We investigated the properties of a piezoelectric tube actuator to determine its suitability for use in a potential fiber positioning system. Our goal was to determine if we could reliably position the tip of the fiber at a specific location, return it there, and maintain it at that location for a period of an hour. The fiber positioning system needs to be precise to 10 microns. Several impediments to this are the piezo's properties of hysteresis and creep. Thus, we needed to design a set up that would allow us to investigate those properties and ways to mitigate them.

The experimental set up consists of a single piezoelectric tube soldered to a mounting board. We ran an optical fiber core through the steel tube that was epoxied inside the top of the piezo. To illuminate the fiber tip we used a contact injector, which is a device that provides light emitting diodes (LEDs) for injecting light into optical fibers without the use of a lens [6]. This injector used deep red LEDs which emit a wavelength of 655nm. Under computer control, we could turn the LED on remotely and control its brightness. We used the injector to illuminate the fiber tip, which allowed us to track the motion of the fiber tip using a camera with a CCD image sensor. This camera, called the Camera Head (A2075) reads out a singular monochromatic CCD and has a short focal length of only 6mm [5]. Because the LED was very strong, the light from the fiber tip would saturate the image sensor even at low power. Consequentially, we were required to place a 10% neutral density filter between the LED and the ferule of the fiber that ran through the piezo and to the tip of the steel tube.

To drive the piezo, we used a piezo amplifier board that takes one input and produces two outputs, one with a gain of +23.6, and the other with a gain of -23.6, which are applied to the piezo's electrodes [7]. The outputs from the piezo amplifier controlled the motion of the piezo in the North-South or East-West direction. We drove the piezo amplifier with a signal generator that was connected to the input, and we used a voltmeter to monitor the voltage applied to the North electrode. For additional tests, we also added a temperature sensor in the enclosure. While tests are run, the experimental setup is covered with a black cloth to block ambient light.

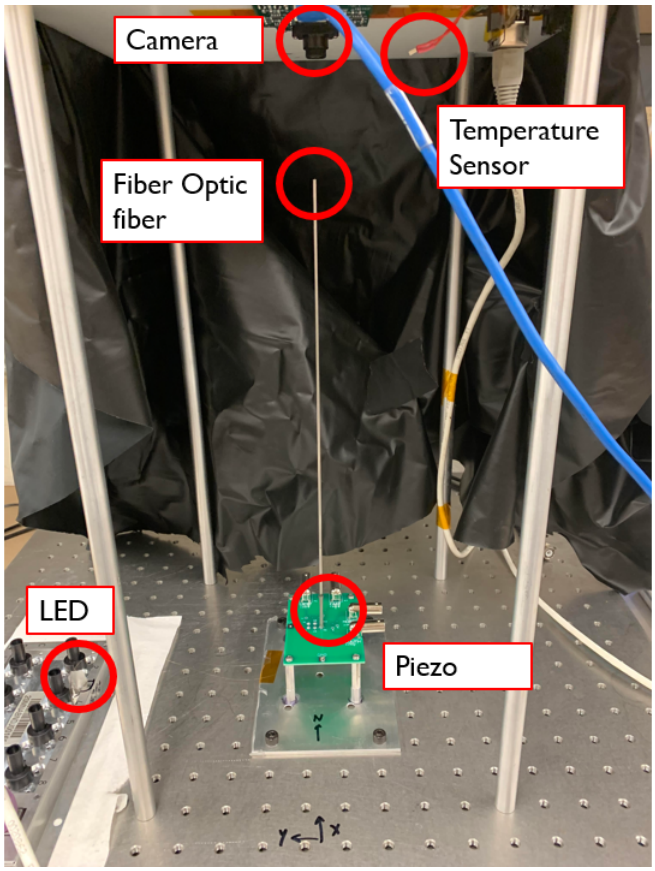


Figure 4: Experimental Set up. The LED is contained within the contact injector. The arrow labeled with an N corresponds to the direction that the piezo moves when a positive voltage is applied on the North-South electrodes. This direction corresponds with the X-direction defined on the CCD when an image is taken. Similarly, when voltage is applied on the East-West electrodes, the piezo moves in the Y-direction.

## 2.1 Issues with Design

When we first began measuring the voltage applied to the piezo's North electrode, we used a voltmeter, A2057V. This voltmeter was created to be used with the Brandeis High Energy data acquisition system [8]. The voltmeter was connected to the output through a resistive divider. However, due to a miscalculation of the resistor values, we accidentally loaded the output of the piezo amplifier. Consequentially, the voltages we measured as applied to the piezo during several experiments are not accurate. These tests include those presented in section 4.4.1 and 4.4.2.

## 2.2 Remote Control Set Up

We later upgraded the experimental set up to allow for full remote control. For this, we used two upgraded A2057 Input-Output heads along with two piezo amplifier

boards. The Input-Output heads allowed us to control the driving voltages for both the North-South and East-West electrodes simultaneously. They also monitor the voltage output on all four electrodes: North, South, East, and West [8]. Furthermore, the issue with the resistive divider loading the output of the piezo amplifier was corrected, allowing for accurate voltage monitoring. However, this set up was only used for one experiment, a creep mitigation test (see section 4.3.2).

# 3 Piezoelectric Tube Actuators

## 3.1 Basics of Piezoelectricity

The piezoelectric effect is the occurrence of an electric charge accumulation on certain solid materials in response to pressure. In contrast, the inverse piezoelectric effect causes certain materials to deform and change in length when an electrical voltage is applied. The piezoelectric effect occurs in monocrystalline materials such as quartz, as well as polycrystalline ferroelectric ceramics [2].

Piezoelectric ceramics have a spontaneous polarization; that is, the positive and negative charge domains are oriented randomly [2]. To make the ceramic macroscopically piezoelectric, a ferroelectric polarization process is required. During this process, a strong electric field of several kV/mm is applied to the ceramic to cause a reorientation of the charge domains. After the electric field is removed, most of the domains retain the new position; however, a small number of the domain walls shift back to their original orientation [2]. Today, piezoelectric technology has a wide field of applications, from use in automotive technology to loudspeakers, to scientific applications such as scanning probe microscopes and fiber positioning systems on spectroscopic telescopes [2].

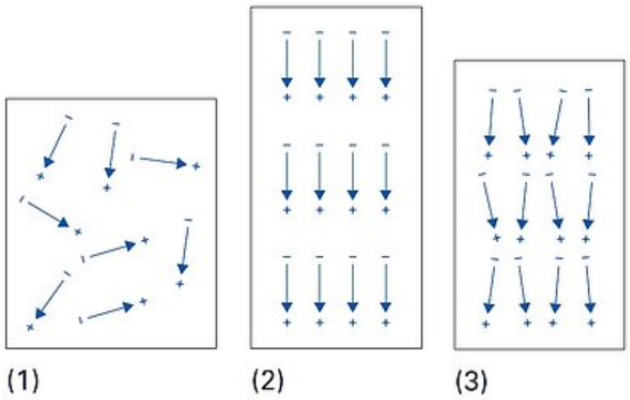


Figure 5: Example of the principle of the ferroelectric polarization done on piezoelectric ceramics to create a macroscopic polarization.(1)The domains are randomly organized. (2) An electric field is applied to the ceramic, uniformly orienting the domains. (3)After the electric field is removed, most of the domains retain the applied orientation [2].

## 3.2 Piezo Characteristics

The piezoelectric actuator used in this experiment was the PI230.94 designed by PI Ceramic. It has a height(h) of 30mm, an outer diameter(OD) of 3.2mm and an inner diameter(ID) of 2.2mm which result in a nominal deflection($x_p$) of $\pm 35\mu$m at the tip of the piezo [2]. It consists of four electrodes arranged in quadrants on the outside that allow it to deflect in both the X and Y direction, as well as an inner electrode which is grounded.

Figure 6: Close up of a piezo electric tube actuator such as those used in this experiment. Two outer electrodes are visible [2].

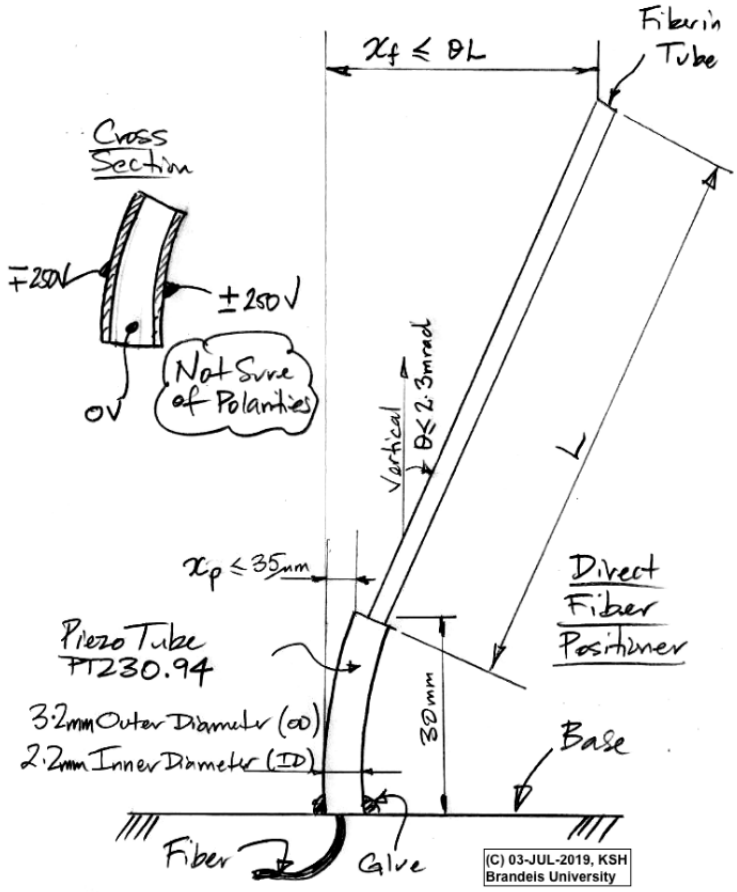


Figure 7: On the left of the image, there is a small cross section diagram of the piezo showing two electrodes which receive voltage, and the inner electrode which is grounded. On the right we have a diagram of fiber tip displacement ($x_f$) corresponding to tube length($L$), and displacement of the piezo tip ($x_p$) [7].

The motion of the piezo is not linear with respect to the voltage applied. One cause of this is hysteresis; the piezo's motion is not only dependent upon the current voltage applied, but also on previous voltages applied. Creep, a change in displacement over time with an unchanged drive voltage, also affects the piezo's motion [2]. Equation 1 is given by the manufacturer to model the creep behavior.

$$\Delta x_p(t) \approx \Delta x_p(t_1)\Big[1 + \gamma log(\frac{1}{t_1})\Big] \tag{1}$$

Here, $t$ is the time from when the voltage is applied, $\Delta x_p$ is the displacement of the piezo tip after the voltage was applied, and $\Delta x_p(t_1)$ is the displacement of the piezo at some time $t_1$. $\gamma$ is the creep factor; its value is dependent upon the material properties of the piezo [2]. We use this equation to model and predict how the piezo will move when an unchanging drive voltage is applied.

### 3.3 Methods

To track the motion of the piezo and fiber apparatus, we took photos of the illuminated fiber tip with the camera. Thus, we could track the motion of the fiber tip's image on the CCD. Then, to determine the motion of the fiber tip in "real" space, we had to determine how far the spot would move on the image sensor with respect to a known change in position of the fiber tip. This is difficult due to the distortion caused by the lens, known as a barrel distortion. However, we assumed that if we positioned the system in such a way that the spot was near the center of the image, and that the fiber tip's motion was parallel to either the X or Y camera axis, then this effect would be minimized. To determine the ratio between motion at the fiber tip and motion on the image sensor, we positioned the fiber tip base in a start position such that the spot was near the center of the image. Then we moved it a known amount with a gauge block. When we compared the displacement in "real" space to the displacement on the image sensor, we found the ratio to be 10 to 1. Therefore a displacement 1$\mu$m of the spot on the image sensor corresponds to 10$\mu$m at the tip of the fiber.

## 4 Results

### 4.1 Range of Motion

The first test we performed was to determine the range of motion at the tip of the fiber. We initially predicted a range of motion of 1.39mm total, as $x_f \leq \theta L$ where $L = 302.5$mm and $\theta = 2.3$mrad. Before we started the experiment, the piezo had been resting with no voltage applied to it for several days. We then applied voltages from +236V to -236V in 23.6V increments to the piezo. Between applying the voltage and taking an image of the piezo, we waited approximately 1 minute. This was done due to initial worries that the fiber would vibrate after a sudden voltage change. Later tests we ran indicated that if the fiber does vibrate after a sudden voltage change, it is undetectable.

We found that in the North-South direction the spot moved 234$\mu$m on the image sensor, corresponding to 2.34mm at the tip of the fiber tip. The same was found in the East-West direction. This was 0.95mm greater than initially predicted. It should be noted that creep had an effect on these measurements, as the piezo continues to move after a constant voltage is applied. The wait time of about a minute from between when the voltage was applied and when the image was taken caused the fiber tip to continue to move, and would create a greater total displacement.

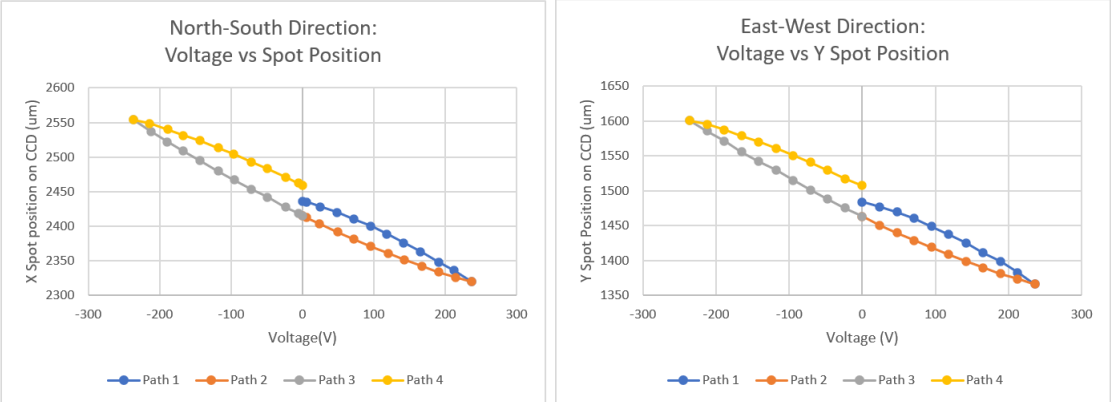


Figure 8: Range of Motion Tests, showing the position of the spot on the image sensor as voltage is applied in the North-South direction (left) and East-West Direction(right).

## 4.2 Hysteresis

As shown from the range of motion tests, the system exhibits hysteresis. Hysteresis is the tendency of a system to retain a "memory" of its previous state, so the physical state of the system lags behind the changes applied to it. Consequently, the deflection of the piezo is not linear with respect to the voltage applied to the electrodes, but follows the curve shown below in Figure 9. Due to hysteresis there are a range of locations the piezo can be at for any given voltage. The greatest of these is at 0V, where we see a difference of 44.1$\mu$m between the location of the image on the CCD during the second path, and the fourth path. This corresponds to 441$\mu$m at the fiber tip. Because this range is greater than the 10$\mu$m precision necessary to control the fiber tip, we need to mitigate hysteresis.

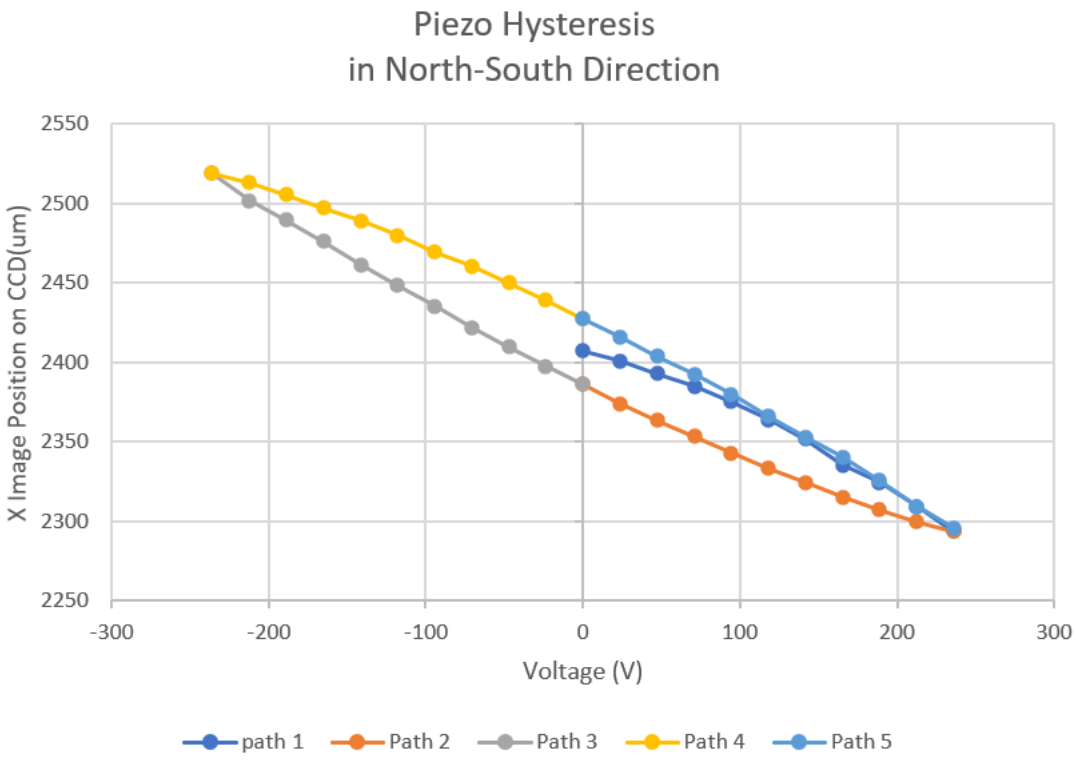


Figure 9: Example of a full Hysteresis Loop, with voltage applied in the North-South direction.

We also wanted to test if the same hysteresis loop would be traced out several times by the piezo. We ran the hysteresis test around again and found that the piezo does indeed retrace the same loop, as shown in the figure 10 below.

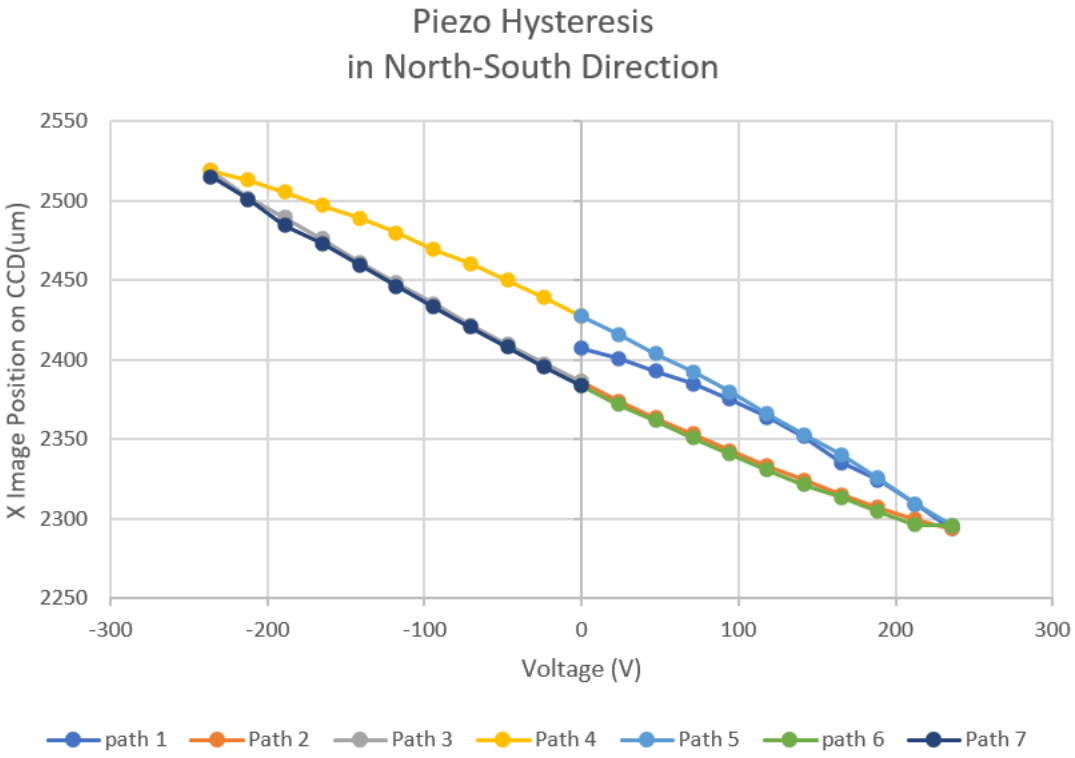


Figure 10: Example of Hysteresis Loop retraced. Path 6 and 7 retrace paths 2 and 3, respectively.

## 4.3 Hysteresis Mitigation

We performed two preliminary investigations into how to mitigate the effects of hysteresis on the system. To show hysteresis mitigation, we wanted to apply some voltage to the piezo and note its location, then apply some intermediate voltages. Then, when we returned to the original voltage, the goal was that the piezo had returned to its original location.

### 4.3.1 Amplitude Modulated Sinusoid

In the first test, we attempted to mitigate hysteresis by applying an amplitude modulated sine wave voltage, specifically a 1Hz sinusoid with an amplitude modulation of 10milliHz. The applied voltage can be modeled by equation 2.

$$V = A \sin\left(2\pi f_m t + \frac{\pi}{4}\right) \sin\left(2\pi f_b t\right) \tag{2}$$

Where V is the output voltage in volts, A is the maximum amplitude in volts, and t is the time in seconds. $f_m$ is the modulation frequency, here 10mHz, and $f_b$ is the base frequency, here 1Hz. An example of how this voltage appeared on an

oscilloscope is shown in Figure 11 below.

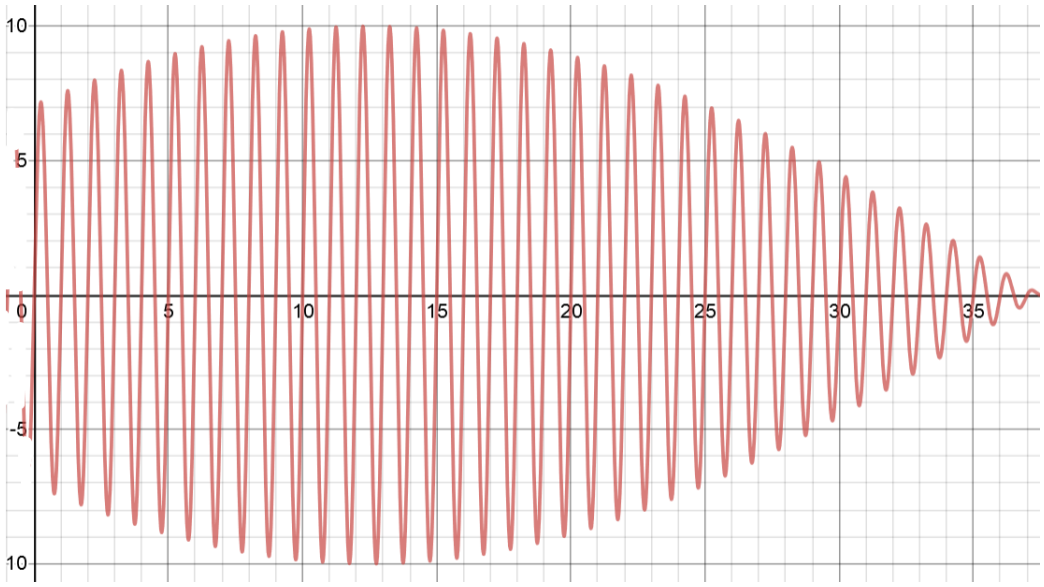


Figure 11: Example of the waveform of the voltage applied to the piezo, graphed from equation 2.

As we applied the voltage, we took an image of the fiber tip as quickly as possible (approximately every 1-2 seconds). It should be noted that because there was no synchronization between the camera and the signal generator, we do not know what voltage was being applied to the piezo at the time the image was taken. Also, because there are sometimes lags with the data acquisition we are not sure if the images were taken at equal intervals. However, we do know when the voltage returned to 0V, as we monitored the voltage applied to the piezo throughout the experiment with an oscilloscope. We took the first location as the home position, and after we applied the sinusoidal voltage, we continued to take images until the voltage returned to 0. The results are shown Figures 12 and 13 below.

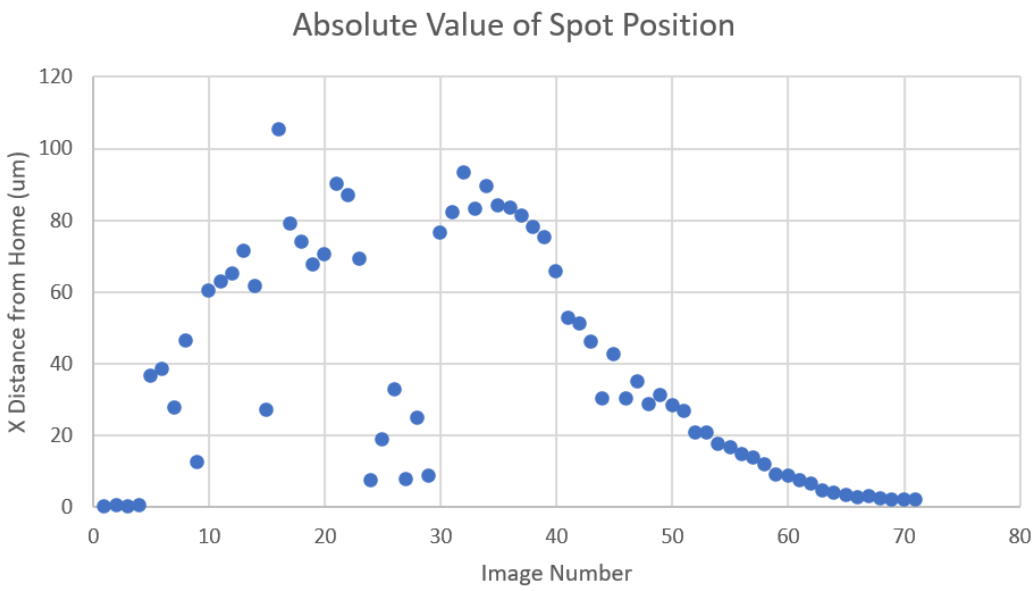


Figure 12: Results of the preliminary hysteresis mitigation test, showing the displacement of the spot position from the home position over the course of the experiment.

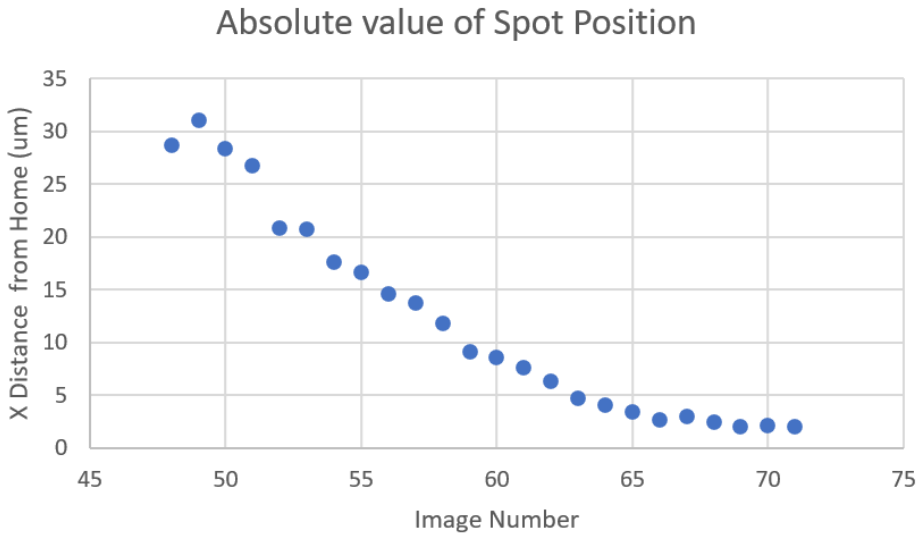


Figure 13: Last twenty-three images of the preliminary hysteresis mitigation test, demonstrating how the image of the fiber tip approaches the home position.

When the peak-to-peak voltage approaches 0V, which is occurring during the image sequence shown in Figure 13, the displacement of the spot returns to within 2$\mu$m from the home position on the image sensor. Thus the fiber tip returns to within 20$\mu$m of the home position. While this does not meet our requirement of 10$\mu$, further testing could be of use to determine the usefulness of this method of hysteresis mitigation. This experiment would especially benefit from repeating it

with the current remote control setup that allows us to monitor the voltage at the time each image is taken.

### 4.3.2 Returning Extrema Test

The hysteresis loop is retraceable, and hysteresis has the smallest effect when the maximum and minimum voltage is applied to the piezo. Therefore we hypothesized that if we applied the maximum voltage to the piezo, then some intermediate voltage, and back and forth again, the piezo would return to the same location. We decided to test this theory by applying +236V and +118 to the piezo (North Electrode) several times, and observing the range the spot position. However, there was a maximum displacement of $9\mu$ on the image sensor when we returned to +118V several times, so we initially thought this theory was incorrect.

However, later on we realized that we had failed to account for the impact of creep on these measurements (see section 4.4). In the first run of this test, we did not control the time between when the voltage was applied and when the image was taken. Thus we ran a second experiment[1] where we attempted to control for this time better. While we could not control for the time between when the voltage is changed and when the image is taken with our current set up, we could specify the amount of time between the images are taken. Therefore, we set a 15 second time interval for image capture. Once we saw that an image had been taken, we would manually change the voltage that was applied to the piezo. In this manner we constrained the time from when the voltage was applied and when the image was taken between 5s and 15s.

Again, we applied between +236V and +118V measured on the piezo's North electrode. This was done manually, over a 24.5 minute period. The displacements on the CCD from the first +236V location and the first +118V location are shown in Figure 14 below.

[1] This was done with the updated experimental setup for remote control.

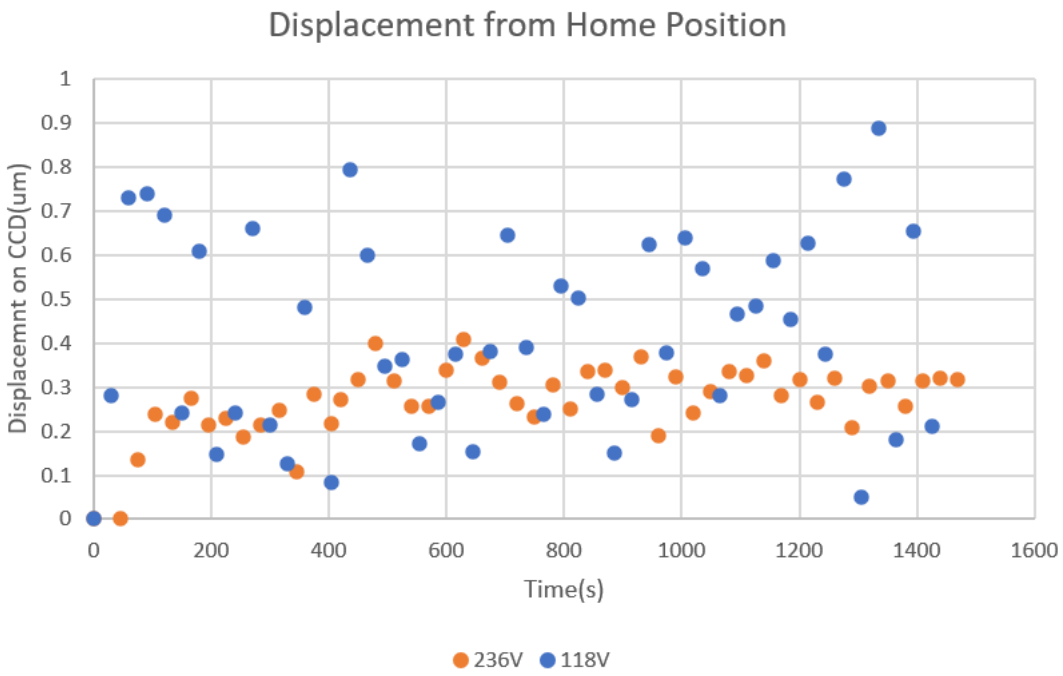


Figure 14: Returning Voltage Test, showing the displacement from the first location of the image on the CCD at +236V and +118V on the North Electrode.

The range of displacements from home at both voltages is within 1$\mu$m on the image sensor, and therefore meets the 10$\mu$m requirment at the tip of the fiber. The standard deviation of the points when +236V is applied to the North Electrode is 0.072$\mu$m while the standard deviation of the points at +118V is 0.221$\mu$m on the image sensor. While this method of hysteresis mitigation needs more investigation at additional voltages, this test suggest that if the time between when the voltage is applied and when the image is taken is controlled, returning to a maximum or minimum voltage may mitigate hysteresis, and cause the fiber tip to return to a constrained location for any given voltage.

## 4.4 Creep

### 4.4.1 Gamma Value

As stated previously, creep is a change in displacement over time with an unchanged drive voltage. In equation 1 $\gamma$, the creep factor, is highly influential in determining the path the piezo will take. Thus, for a variety of input voltages into the piezo amplifier, $\pm$10V, $\pm$9V, $\pm$5V, and $\pm$2V, we observed how the position changes over time when the piezo is driven with a step voltage from 0V to the set voltage over about an hour. For these tests we will give the voltage that was applied into the piezo amplifier, as our voltage readings on the piezo are inaccurate

due to loading on the piezo amplifier output.

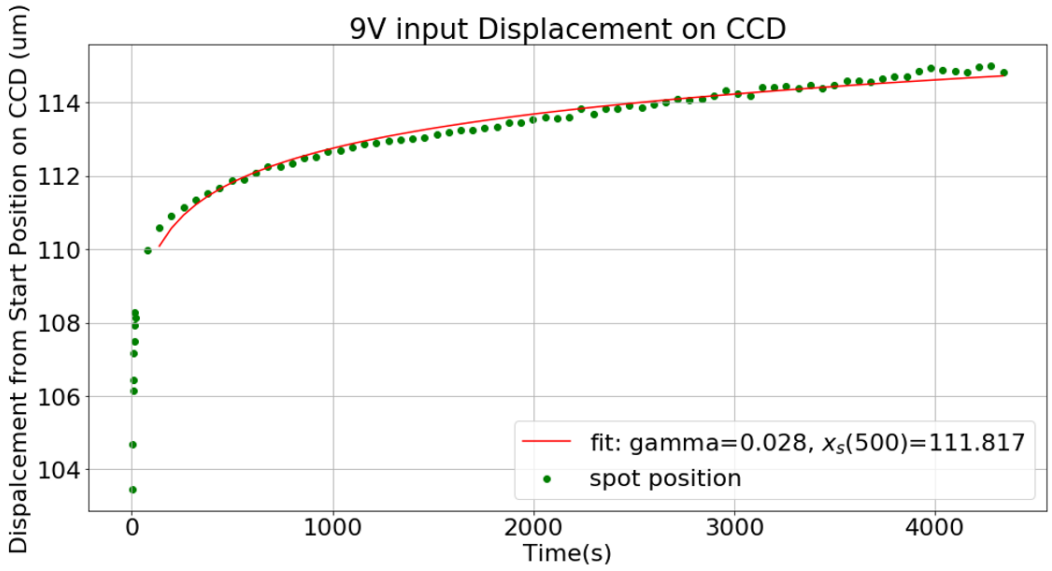


Figure 15: Displacement due to creep with 9V input to the piezo amplifier. We fit for both $\gamma$ and $x_s(500)$, which is the position of the spot on the image sensor at 500s.

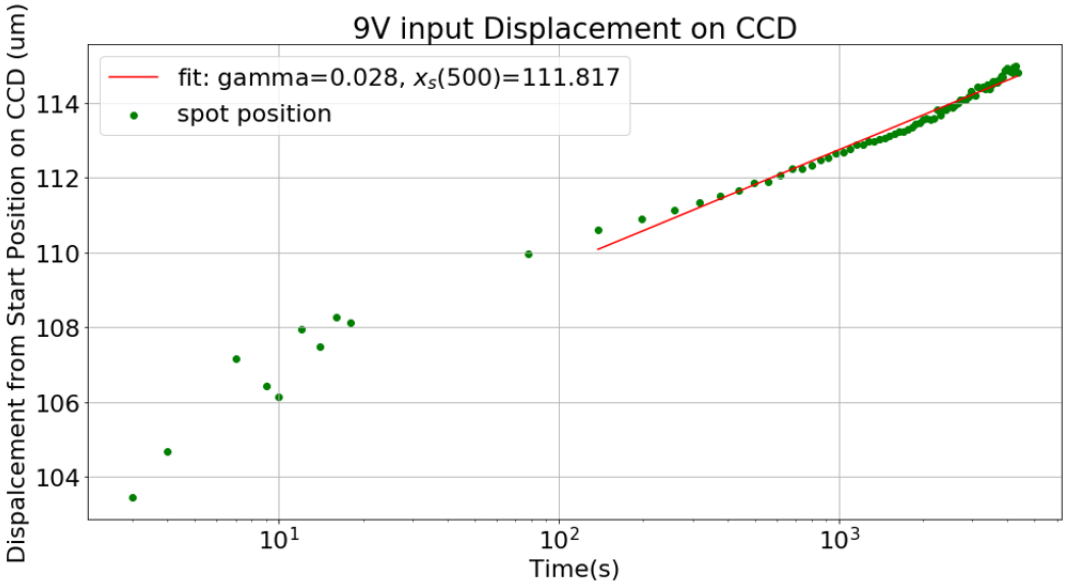


Figure 16: Displacement due to creep on a log plot.

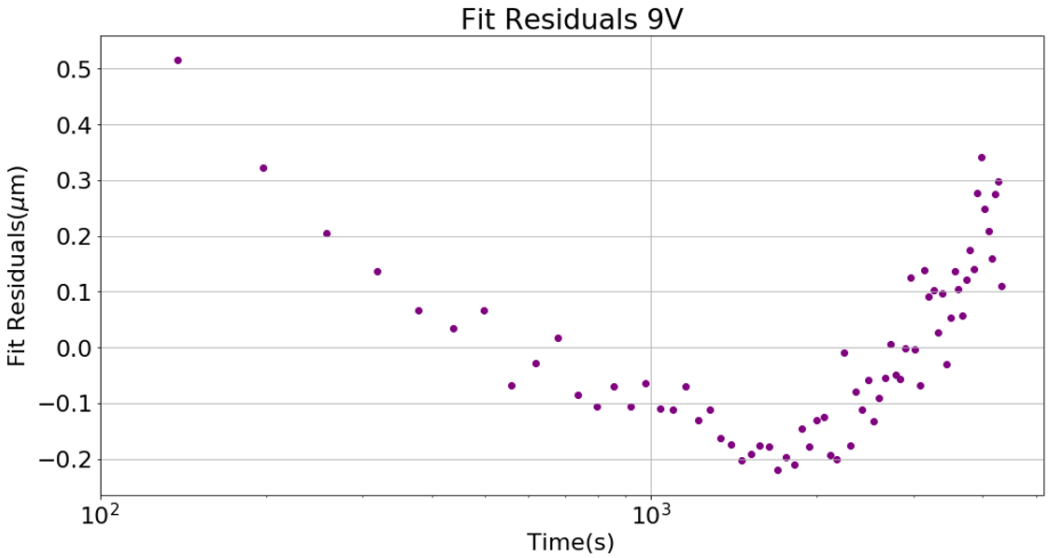


Figure 17: Creep residuals on the CCD, with a standard deviation of 0.16$\mu$m.

To determine how to properly fit for $\gamma$, we used python's scipy.optimize curve fit function. We fitted for both $\gamma$ and $x_s(500)$, which is the displacement of the spot on the image sensor at 500s after the voltage is applied. It corresponds to the displacement of the piezo tip, $\Delta x_p(t_1)$ in equation 1, where $t_1$ is 500s. Taking this fit we also excluded all points before the 100s mark from the fit.

| Input Voltage(V) | $\gamma$ |
|---|---|
| 10 | 0.026 |
| 9 | 0.28 |
| 5 | 0.056 |
| 2 | 0.067 |
| -2 | 0.024 |
| -5 | 0.033 |
| -9 | 0.028 |
| -10 | 0.029 |
| Average | 0.036 |
| Standard Deviation | 0.015 |

Table 1: Table listing the voltage applied to the piezo amplifier, and the value of gamma acquired through a fitting function.

While the gamma values for an input voltage of 5V and 2V are outliers, the remaining gamma values appear to cluster closer together. This test should be repeated to improve our measurements of gamma at different voltages and with a different step voltage, for example from -10V input to the set voltage. Performing these new tests should help us to better understand creep.

### 4.4.2 Creep Mitigation

Since creep is a product of a static drive voltage, we hypothesized that a changing voltage applied to the piezo would help mitigate creep. Therefore we applied a ramping down voltage with a period of 3.60ks(1 hour), an amplitude of 250mVpp, a DC offset of 9.750V and a syme of 0%.

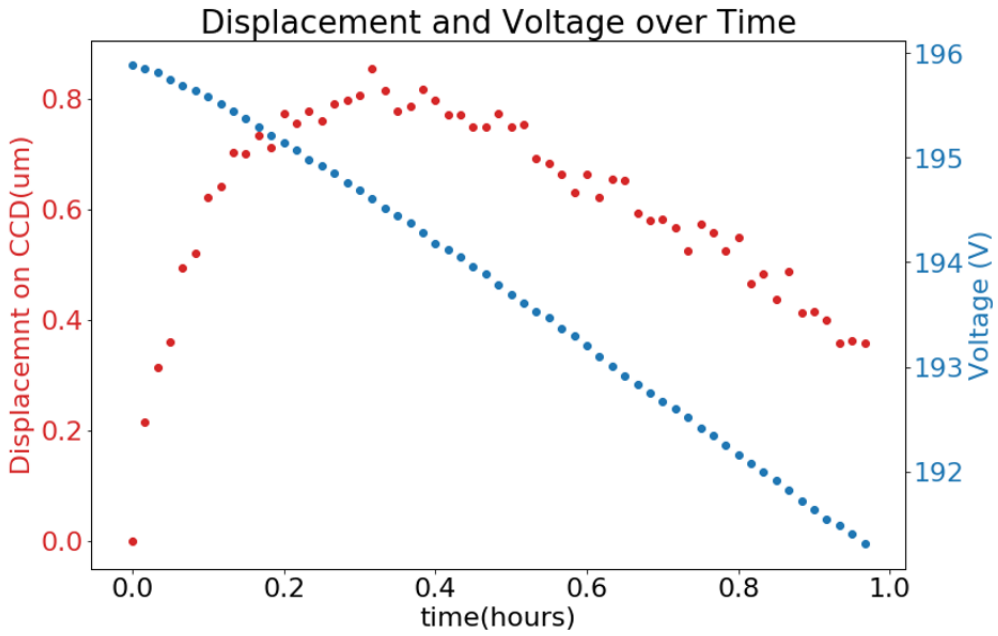


Figure 18: Creep Mitigation Test. In blue, we have the ramping voltage, from 185V to 181V. In red we have the displacement of the spot on the image sensor. It should be noted that when measuring the voltage we were in inadvertently loading the circuit, thus the voltages measured are not accurate, although the shape of the curve is.

Over the course of an hour, the spot moved a maximum of 0.85$\mu$m from the home position, which is 8.5$\mu$m at the tip of the fiber. This is less than the 10$\mu$m necessary, and is an encouraging result as we could possibly use this method to mitigate creep at all voltages. However, further tests must be done to confirm. We suggest that this test be done at a range of voltages to determine if the same ramping voltage can be used at all input voltages, or if more or less ramping is needed.

We also suggest that a logarithmic voltage signal be applied to the piezo. This would hopefully counteract all creep completely, resulting in 0 displacement from the home position over the course of an hour.

## 4.5 Temperature

During some initial, long period tests we observed motion of the fiber tip when no voltage was being applied to the piezo. Therefore we added a temperature sensor to the set up to monitor both the displacement and temperature over periods of at least 24 hours. The first test was over a 25 hour period, and the second was over 60 hours.

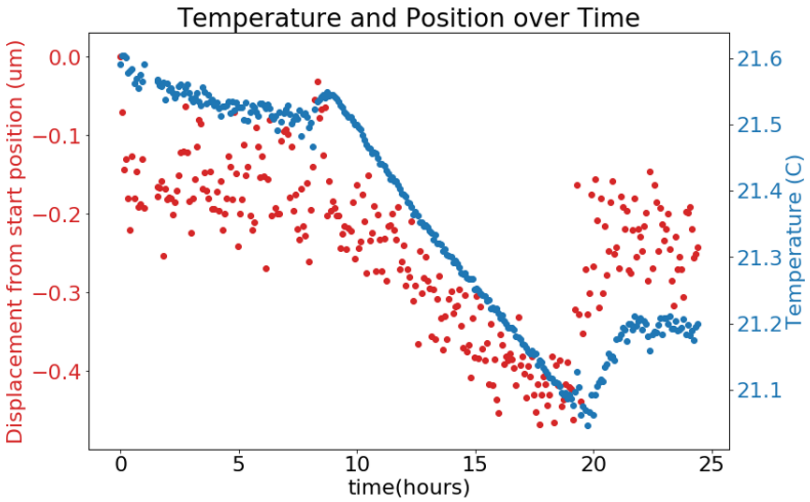


Figure 19: Temperature and image displacement on the CCD test 1. Over the course of 25 hours we see a maximum displacement of 0.45$\mu$m on the CCD, and a max change in temperature of 0.5 °C.

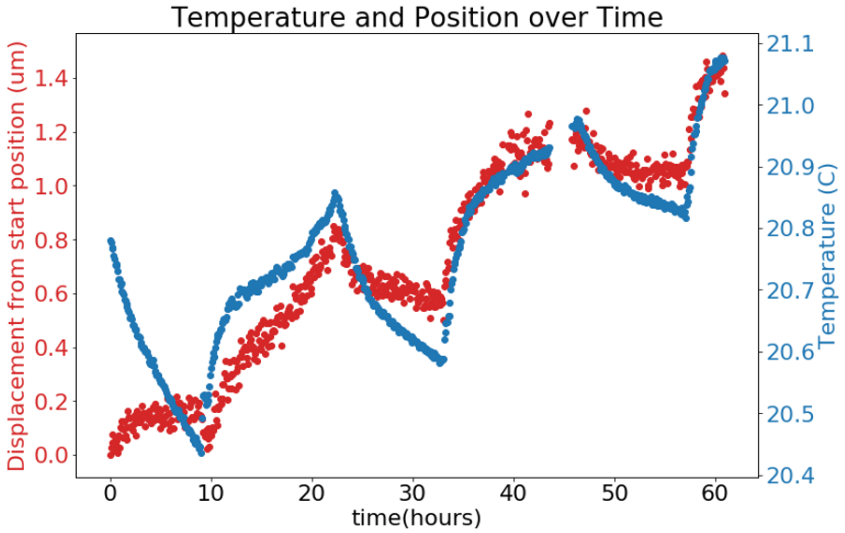


Figure 20: Temperature (in blue) and image displacement on the CCD (in red) test 2. Over the course of 60 hours we observed a maximum displacement of 1.4$\mu$m on the CCD, and a maximum change in temperature of 0.7°C.

There is a clear correlation between the displacement and temperature, however it is unclear what this precisely the relationship is. The first test appears to indicate a relationship of $0.30\pm0.16\frac{\mu m}{^\circ C}$, where the second test indicates $2.16\pm0.55\frac{\mu m}{^\circ C}$. Future testing must be done to determine the exact relationship between temperature change and spot displacement on the image sensor. However, these results indicate that whatever enclosure the fiber positioning system is housed within needs to be sufficiently temperature controlled, perhaps to within 0.5°C.

# 5 Conclusions and Prospects

Over the course of this project, we studied the range of motion, hysteresis, and creep of the piezoelectric tube actuator. We found that the range of motion exceeded what was expected, at a range of 2.34mm at the fiber tip. With respect to hysteresis, we observed that it will return to similar positions at each voltage when the loop is retraced. We also investigated two possible methods of hysteresis mitigation. The first method was to apply an amplitude modulated voltage to the piezo. This test resulted in the fiber tip returning to within 20microns of the original position. While this does not meet the necessary requirements, future studies of this method could be enlightening. The second hysteresis mitigation method was to apply the max or min voltage to the piezo, and then return to some intermediate voltage. The results of this test showed that at both +236V and +118V, the range of the displacements from the home position was less than 10$\mu$m at the fiber

tip. We found that at the max voltage of +236, the standard deviation of the fiber tip's location was 0.72$\mu$m, and at the intermediate voltage of 118V, the standard deviation is 2.21$\mu$m at the fiber tip. While this is only one example of this method, it shows promise as the range of position is within our specification of 10$\mu$m.

Our investigations of creep led us to fit our data for $\gamma$ in Equation 1, the creep factor, for various voltages. We hope that a better understanding this creep factor will allow us to control for creep and mitigate it. We performed one preliminary test into creep mitigation, and found that by applying a ramping down voltage over the period of an hour, we were able to keep the range of the fiber tip to within 9 microns. This is also within our 10 micron requirement. While this is extremely encouraging, further testing is necessary at a variety of input voltages.

Our final test was to investigate how temperature affected the experimental set up. We observed the fiber tip over a period of both one day and two days, and found that there is a clear correlation between temperature and tip movement. While future tests are necessary to determine this exact relationship, it currently appears that any fiber positioning system must be temperature controlled to within 0.5°C.

## 5.1 Future Prospects

We recommend repeating the majority of these tests for further study and confirmation with the improved remote control experimental setup. For the hysteresis tests, we recommend that the returning voltage tests be repeated for variety of intermediate voltages. For our creep mitigation tests, we recommend that the ramping voltage test is repeated at a variety of input voltages as well to determine if a smaller or larger amplitude is necessary to constrain the fiber tip's motion to within 10microns. We also recommend applying a logarithmic voltage signal to directly counteract the creep and lessen it's effect over the course of an observation. Lastly, all of the tests in this experiment were run on a single piezoelectric tube actuator. We believe it would be beneficial to repeat these tests on several different piezos as well with several piezos soldered to the mounting board simultaneously.

# References


[1] BROWN, D. M., ET AL. Starbug fibre positioning robots: performance and reliability enhancements. *Advances in Optical and Mechanical Technologies for Telescopes and Instrumentation* (Aug 2014).

[2] CERAMIC, P. *Piezoelectric Actuators*, 1 ed. PI Ceramic GmbH, Lindestrasse, 07589 Lederhose, Germany, Feb. 2019. A full MANUAL entry.

[3] COLLABORATION, L. LSST Technical Details: Focal Plane Requirments, Feb 2020.

[4] ELLIS, R., ET AL. SpecTel: A 10-12 meter class Spectroscopic Survey Telescope, 2019.

[5] HASHEMI, K. Camera Head (A2075) Manual, 2018.

[6] HASHEMI, K. Contact Injector (A2080) Manual, 2018.

[7] HASHEMI, K. Fiber Positioner Circuits (A2089), 2020.

[8] HASHEMI, K. Input-Output Head (A2057) Manual, 2020.

[9] LEITNER, D., ET AL. Dark Energy Spectroscopic Instrument (DESI) Fiber Positioner Production, 2018.

[10] MARTINI, P., ET AL. Overview of the Dark Energy Spectroscopic Instrument, 2018.

[11] SCHLEGEL, D. J., ET AL. Astro2020 APC White Paper: The MegaMapper: a $z > 2$ spectroscopic instrument for the study of Inflation and Dark Energy, 2019.

[12] SHEINIS, A., ET AL. Advances in the Echidna fiber-positioning technology. In *Advances in Optical and Mechanical Technologies for Telescopes and Instrumentation* (2014), R. Navarro, C. R. Cunningham, and A. A. Barto, Eds., vol. 9151, International Society for Optics and Photonics, SPIE, pp. 638 – 660.

[13] SMEDLEY, S., ET AL. Sphinx: a massively multiplexed fiber positioner for MSE, 2018.

[14] STUBBS, C. W., AND HEITMANN, K. Report on LSST Next-generation Instrumentation Workshop, April 11, 12 2019, 2019.

[15] TEAM, T. M. S., ET AL. The Detailed Science Case for the Maunakea Spectroscopic Explorer, 2019 edition, 2019.

# Appendix

In this appendix we have provided a chart of the characteristics of the piezo used in this experiment. We also provide additional graphs that provide more insight into several creep factor measurements.

| | DimensionsL × OD × ID | Max. operating voltage | Electrical capacitance | Max. axial displacement | Max. XY deflection |
|---|---|---|---|---|---|
| | | *V* | *nF* | *µm* | *µm* |
| PT230.94 | 30 mm × 3.2 mm × 2.2 mm | ±250 | 4 × 2.1 | ±4.5 | ±35 |

Figure 21: Piezo characteristics including the dimensions, max operating voltage, and max XY deflection [2]

Below are several plots where we see motion of the spot on the image sensor due to creep. The first set (Figures 22-24) are when +10V is applied into the piezo amplifier, resulting in 236V on the piezo. This tests were done with the remote control set up, therefore they were not included with the data from the previous set up. As you can see in Figure 24, the standard deviation of the residuals is 0.083$\mu$m, almost half those shown in Figure 17. The fit returned a creep factor of $\gamma = 0.016$. It is interesting that the value of the creep factor that fitted for with this data differs so greatly from the values presented in Table 1. While there is some difference in the voltage that was applied to the piezo, it is surprising that it would cause such a large change in the creep factor value. Additional testing should be done to investigate this further.

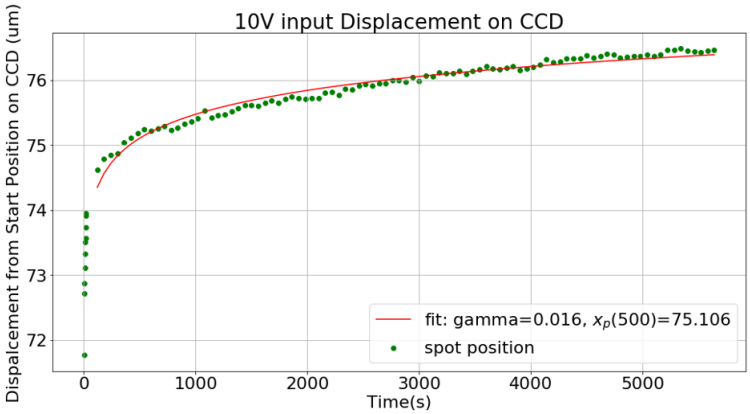


Figure 22: Displacement on the CCD with a 10V input driving voltage, demonstrating creep.

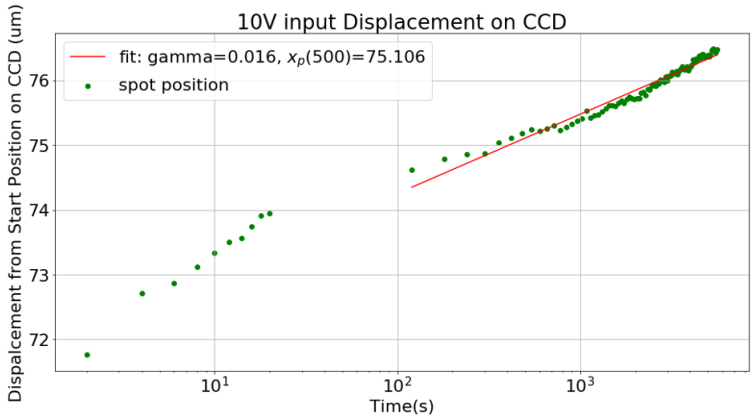


Figure 23: Displacement with a 10V input driving voltage on a log Plot.

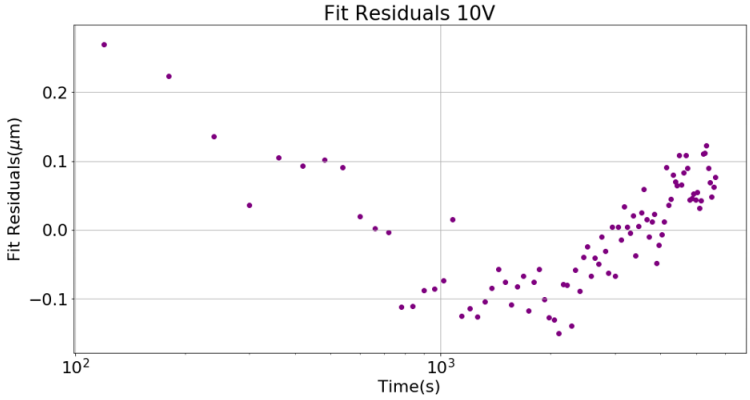


Figure 24: Fit residuals for a 10V input voltage on the CCD.

In the second set of graphs, we display the data from 2V being applied to the amplifier, this was done with the original set up. 2V was one of the tests in which the creep factor was an outlier, with $\gamma = 0.67$. These graphs are presented to show that this outlying $\gamma$ is not due to poor fitting, as the standard deviation of the fit residuals is $0.09\mu$m.

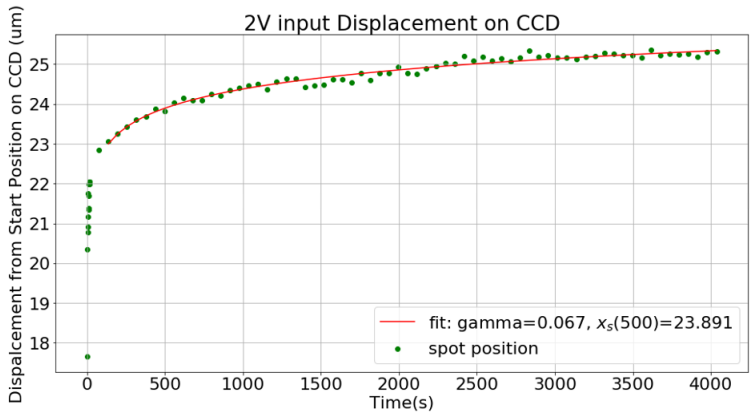


Figure 25: Displacement, demonstrating creep, for a 2V driving input.

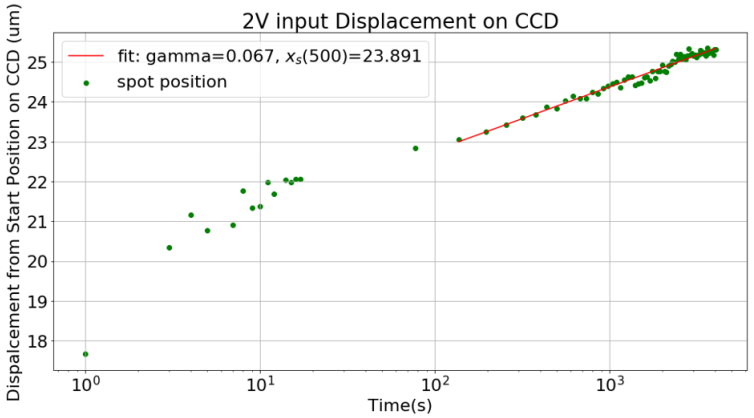


Figure 26: Displacement on a log Plot, for a 2V driving input.

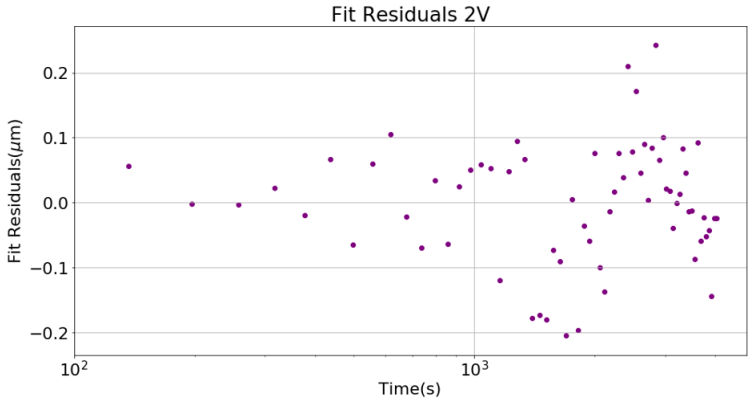


Figure 27: Creep residuals on the CCD for 2V driving input.